Journal of Materials Chemistry A

Accepted Manuscript

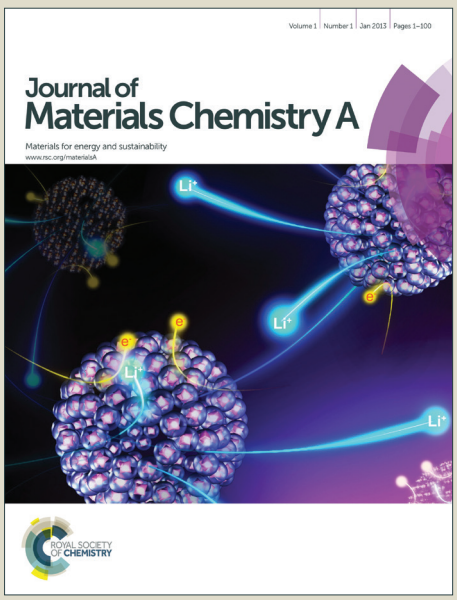

ROYAL SOCIETY OF CHEMISTRY

www.rsc.org/materialsA

Electro-active Shape Memory Composite Enhanced by Flexible Carbon Nanotube/ Graphene Aerogel

Xuefa Liu[1†], Hua Li[1†]*, Qingping Zeng[1], Yangyang Zhang[1], Hongmei Kang[1], Huanan Duan[1], Yiping Guo[1], Hezhou Liu[1]*

[1]State Key Laboratory of Metal Matrix Composites, School of Materials Science and Engineering, Shanghai Jiao Tong University, Shanghai 200240, China

Corresponding author: Hua Li, lih@sjtu.edu.cn; Hezhou Liu, hzhliu@sjtu.edu.cn.

Tel.: +86 021 34202549.

Postal Address: Room 331, Material Building D, Shanghai JiaoTong University, Dongchuan Road No. 800, Shanghai, 200240, China.

[†]X. Liu and H. Li contributed equally to this work

ABSTRACT

In this manuscript we present a novel, shape memory aerogel/epoxy composite structure composed of a reduced carbon nanotubes and graphene compound aerogel as scaffold, and epoxy resin as matrix. The composite was prepared via a vacuum infusion method and -to the best of our knowledge- it represents the first instance of shape memory effect directly driven by an electrical field observable in the polymer-infused conductive carbon scaffolds. Furthermore, the composite material obtained displays a high conductivity (i.e., up to 5.2 S/m). In the manuscript it is shown that the composite's high conductivity can be attributed to the built-in 3D network of the thermally-reduced graphene and carbon nanotubes compound aerogel which display high conductivity (16 S/m) coupled with low density (6 mg/ml). The composite material presented in this work is likely a suitable candidate for applications requiring polymer-infused conductive aerogels such as electromagnetic shielding, actuators and thermal sensors.

KEYWORDS：carbon nanotube and compound aerogel，shape memory composite

1. INTRODUCTION

Carbon nanotubes and graphene are two intensively studied novel functional materials in the carbon material family. Graphene, which is composed of a two-dimensional, thin carbon atom framework, is known for its outstanding electrical, mechanical, and thermal properties. Carbon nanotubes (CNTs) can be viewed as a wrapped single or multiple graphene sheets with a tube-like shape. Graphene and carbon nanotube have found their applications in many fields such as catalyst support [1, 2], environment protection [3, 4], and supercapacitors [5]. Reports on their applications in performance materials also prove that they are effective fillers for composites thanks to the ability

to enhance the mechanical and electrical properties of the matrices [6]. Regretfully, the poor dispersion characteristics of graphene and carbon nanotubes in polymer matrix has currently limited their application in performance materials[7]. To date, various methods have been proposed to improve the dispersion of these materials in polymer matrices; among them, functionalization is the most recurrent one[8, 9]. Effective as functionalization to better disperse graphene and carbon nanotubes into different matrices, but the high interlayer contact resistance caused by functional groups has limited their as conductive filler [10]. Therefore preparing highly conductive graphene and carbon nanotubes structure is very crucial for qualifying graphene as scaffold for conductive composite.

Recently, the emergence of aerogels composed of graphene and carbon nanotubes has paved the road to the fabrication of highly conductive composites in light of the high conductivity and compatibility of the aerogels with organic materials [11]. Yang et al. [12], have developed a vacuum infusion method to fabricate highly conductive epoxy composites with their conductivity largely enhanced by the hydrothermally-obtained graphene aerogels. Although aerogels prepared by the hydrothermal method are often stiff enough to bear up to 10 times of their own weight [13], their stiffness and the possibility of failure in deformation process hinder their applications as effective conductive fillers for shape memory composites.. Herein, we report a novel method for the manufacturing of carbon highly conductive and flexible nanotubes and graphene compound aerogels via freeze-drying combined with annealing. The so obtained aerogels, which represents the basic scaffolds of the proposed composite structure, were subsequently impregnated with the shape memory epoxy resin (SMER) to fabricate the final aerogel/SMER composites. The shape memory composite thus obtained represents a 3D scaffold and shape memory polymers (SMPs) that can

respond to stimulus by recovering from its temporarily fixed second shape in the presence of electrical field. Unlike the matrix material alone, it has the advantage that no heat source aught be applied in the shape recovery process[14]. Compared with electro-activate shape-memory composites filled with nanocarbon particles or short carbon fibers, the filler content of our composite is reduced by 90 percent[15]. Furthermore, none obvious change in glass transition temperature is found for the composite. The obtained composites also showed a good shape memory effect with the shape recovery process being triggered by directly connecting the composites to a circuit with relative low voltage (i.e., approx. 60 volts).

Method

Preparation of graphene oxide (GO)

GO was prepared by modified Hummers method[16]. Typically, 1 g graphite powder and 0.5 g of sodium nitrate was mixed with 92 mL concentrated sulfuric acid in a 250 mL flask. The mixture was stirred for 0.5 h in an ice bath. Then 3 g potassium permanganate was carefully added to the suspension under vigorous stirring. The mixture was first kept at 20 ºC in an aqueous bath, then the temperature was increased to 35 ºC followed by a continuous stirring for 1 h. After that, 92 mL deionized (DI) water was slowly added to the mixture. The diluted suspension was stirred for another 30 min before 20 mL H_2O_2 (30%) and 280 mL DI water being added to the mixture. Eventually, the mixture was vacuum filtered and washed with 6% HCl and DI water for several times. The washing process was repeated until the pH of the solution became neutral.

Preparation of multi-wall carbon nanotube (MWCNT) oxide

MWCNT oxide was prepared through a standard technique.. 1 g MWCNTs were mixed with a mixture of 100 ml concentrated H_2SO_4 and HNO_3 (3:1 by volume) and the mixture was stirred and refluxed for 8 h at 60 ºC. Then 300 ml DI water was added to dilute the mixture. The diluted mixture was then filtered through a PTFE membrane with an average pore size of 0.45 μm and washed with DI water for several times until the solution became neutral.

Preparation of CNT and graphene compound aerogel

The CNT and graphene compound aerogel was prepared by a freeze-drying combined with annealing. Firstly, MWCNTs oxide and GO with a mass ratio of 1:5 to 4:5 were dissolved in DI water with the concentration of GO being 2 mg/ml. After the thorough dissolving of MWCNTs oxide and GO, polyvinyl alcohol (PVA, 1 wt%) was added to the mixture and the mass ratio of PVA and DI water was 1:100. Ethyl alcohol was added to suppress the expansion of the mixture when frozen. The compound aerogels formed after the drying process were subsequently annealed by an alcohol blast burner in N_2 atmosphere to pyrolyse PVA and restores the structure of MWCNTs and graphene oxide. Aerogels obtained after annealing were highly compressible and conductive.

Preparation of electro-active shape memory composite

The composite was prepared by vacuum infusion method. Firstly, the obtained CNTs/graphene aerogel would be place in a tin foil mold which was a little bigger than aerogel. Secondly, the aerogel contained in the mold and the mixture of epoxy resin (E-51) and its curing agent DDM (4,4'-diaminodiphenyl methane), would be place into a vacuum drying chamber to be heated at 120℃ together. Finally, the liquid of epoxy resin and its curing agentwould be cast into the mold and the chamber would be vacuumed for about 20 minutes under the same temperature.

Preparation of bended rectangular composites

Shape fixation of sample in rubbery state was carried on an iron cylinder with a diameter of 55 mm and the bending angle was 90 degrees. To keep the precise of bending angle, an angle bracket was applied to fix samples.

Characterizations

The morphology of the as-prepared aerogel was characterized by SEM (Sirion 200, FEI, USA) and the accelerating voltage was 10 kV. High resolution transmission electron microscopy (HR-TEM) using JEOL JEM-2100F with an accelerating voltage of 200 kV.

Fourier transform infrared spectroscopy (FTIR) using BRUCK EQUINOX55 was performed to characterize the effect of oxidation process on graphene and CNTs Elemental analysis was carried on X-ray photoelectron spectroscopy (XPS) using Kratos AXIS ULTRA DLD to verify the existent of chemical bonds of GO before and after reduction. Carbon atom framework, before and after reduction, was characterized by dispersive Raman microscope（RAM, Senterra R200-L, GER）using a 532 nm laser.

Atomic force microscope (AFM) characterization of GO was performed on an Environment Control Scanning Probe Microscope (Nanonavi E-Sweep, SEIKO, JPN) The sample was prepared by dropping a dilute solution(0.2 mg/ml) of graphene on mica sheet.

Compression tests were carried on a materials testing machine (BTC-T1-FR020 TN.A50, Zwick, GER). The compressing speed in high strain (90%) was 6 mm/min and sample tested was a cylinder (diameter and height corresponds to 36 mm and 12mm respectively).The sample tested in the cyclic compression was the same as high strain compression and the load/unload speed was 60 mm/min.

Dynamic mechanical analysis (DMA) was carried out on a DMA 8000 analyzer (PerkinElmer, USA), using a 3 point bending mode at a heating rate of 3 °C/min from 20 to 120 ℃ and at a frequency of 1 Hz. The loss and storage modulus for specimen size 20 × 7× 4 mm (length × width × thickness) was tested.

Conductivity test of aerogel and composite was performed on a 4-point probes resistivity measurement system (RTS-8, PEOBES TECH, CHN) and the operating current range was 0~10 mA. The aerogel and composite sample were both rectangular (length × width × thickness correspond to 90 × 15 × 7 mm).

Shape recovery experiments were conducted on a DC Power (DH1765, DAHUA ELECTRONIC, CHN) and the voltage was set to 60V. Sample tested was rectangle sample (length × width × thickness correspond to 90 × 15 × 7 mm) with two ends coated by conductive adhesive (mixture of Ag particles and epoxy resin). To facilitate the testing process cooper wires were fixed at the other ends of the sample during the curing process of conductive adhesive. An iron cylinder with a diameter of 55 mm was applied in the bending process of samples. The bending angle of every sample was 90 degrees. The recovery process was recorded by a video camera and the angle of the sample in the recovery process was monitored by measuring the shot video with the help of a protractor every 3 seconds.

Surface temperatures of composites were monitored by a thermal infrared imager(MA30, Magnity Electronics, CHN) with temperature range of -20~150℃ (maximum 240 ℃) and accuracy of 0.1 ℃

RESULT AND DISCUSSION

Direct casting seems to be the desirable way to fabricate epoxy-infused aerogel nano-composites since the graphene aerogel is super-hydrophobic and compatible

with various organic reagents. However, the structural strength of composites prepared by directly casting is not comparable to that of the pure epoxy resin due to the pores formation during the mixing process. Therefore, the vacuum infusion technique was introduced to facilitate the mixing process of aerogel and epoxy resin and eliminate undesirable pores. Furthermore, the infusion process was found harmless to the overall structure of aerogels as the overall volume and shape of the aerogels were retained after the curing process(Fig.1).

After oxidation process, the formation of the CNTs and graphene oxide were confirmed by Fourier Transform Infrared Spectroscopy (FTIR). As shown in Fig.2, the peak at 3400 cm^{-1} attributed to the vibration of –OH band,the peaks at 2920 cm^{-1} and 2860 cm^{-1}attributed to symmetry and asymmetry vibration of $–CH_2–$ bonds and the specific absorption peak of C=O bond peak at 1720 cm^{-1} are strong indications that the carbon nanotubes are successfully oxidized. The peak at 1620 cm^{-1} for graphene and the peak at 1598 cm^{-1} for CNTs oxide correspond to the vibration of the C=C bond, a symbol of the original carbon atom framework, indicating that oxidation process would not thoroughly disrupt the original structure of graphene and carbon nanotubes[17].

Dispersion test was carried out to verify the dispersion stability of the CNTs oxide in water. Ultrasonic treated mixtures of oxidized and pristine CNTs with a same concentration of 2mg/ml contained in sample vial were placed in a glass cabinet for 48 hours. Images of the CNTs oxide and pristine CNTs in water before and after the ultrasonic bath step are shown in Fig.3a. A series of CNTs oxide mixtures of different concentration ranging from 0.5mg/ml to 3mg/ml were also placed for 48 to test the dispersibility of CNTs oxide in water. The result showed the maximum solubility of the CNT oxide was found to be about 2 mg/ml.

The conductivity of aerogels are determined by the contact resistance generating from stacking of multiple or single-layer graphene sheets with different thicknesses during the formation process of 3D structure of aerogels. According to Nirmalraj et al[18], stacking made up of thicker graphene sheets will have higher contact resistance. Thus, it is paramount to obtain single-layer graphene sheets in order to decrease the thicknesses of stacking and achieve high conductivity. To obtain single-layer graphene sheets, oxidation process was applied and atomic force microscopy (AFM) was used to measure the thickness of the graphene oxide (GO) obtained. As it can be seen from the image shown in Fig.3b, the thickness of our graphene oxide estimated is 0.88 nm. Compared with the normal thickness of graphene (0.4 nm[19]), single-layer graphene oxide was success obtained.

Structure and element change of the graphene before and after the annealing process was characterized by X-ray photoelectron spectroscopy (XPS) and Raman spectroscopy (Fig.4). As clearly shown in Fig.4a, a sharp peak at 532.4 eV assigned to O1s is present before annealing and the concentration ratio of C/O was found to be 0.7[20]. After annealing the sharp peak at 532.4 eV had disappeared and the C/O concentration ratio had increased to 16.7. The large increment in C/O concentration and the disappearance of O1s peak are clear indications that most functional groups were successfully eliminated during the annealing process. Detailed structure variations of carbon atoms were also characterized by XPS as shown in Fig.4b and 4c. Before thermal reduction, three kinds of carbon atoms appeared in the spectroscopy. After the thermal reduction, only one prominent peak present at 284.5 eV(absorption peak sp^2-hybridized carbon atoms) left, indicating an excellent structural recovery of the oxidizedcarbon. Raman spectroscopy data shown in Fig.4d also validated the same result as the intensity ratio between the 1587 cm^{-1} peak (corresponding to the

sp^2-hybridized carbon) and 1350 cm^{-1} peak (corresponding to the sp^3-hybridized carbon) increased from 1.17 to 1.36 [21] . The results gain from XPS and Raman spectroscopy strongly prove that the annealing process is very effective in restoring the original structure of the graphene.

The mixing state of CNTs oxide and GO mixture for the preparation of the compound aerogel was characterized since their compatibility matters whether we can obtain aerogel with homogeneous composition. The result is shown in Fig.5.Fig.5a is the TEM image of mixing state of CNTs oxide and graphene oxide in water and it shows that oxidized CNTs are randomly coated to the sheets of the graphene oxide. The same result can also be observed by SEM images of CNTs/graphene aerogel as shown in Fig.5b.

After annealing the densities of obtained aerogel were caculated by dividing their masses with corresponding volumes, the result shows that the densities of aerogels will increase from 5 mg/ml to 8 mg/ml when CNTs/graphene ratio increased. SEM images of prepared aerogels are shown in Fig. 6 and their corresponding constituents before annealing are reported in table 1 . As shown in Fig.6, the 'as prepared', thermally-reduced carbon nanotubes/graphene compound aerogels display similar 3D pore structures Pores of different sizes ranging from 10 μm to 50 μm could be found in our aerogels. However, no relationship between pore size and different CNTs/graphene compositions has been found. Reasonable explanation for this phenomenon is that CNTs coatedgraphene oxide sheets and PVA would be pushed together by ice crystals and form the original pore structure of aerogel in the freezing process and the preformed pore structure would be preserved by theπ-π stacking of reduced during the pyrolyzation of PVA.

The question of whether aerogel can recover its original structure after deformation is

crucial to qualify potentially successful fillers for applications such as shape recovery composites as ideally composites will not suffer from the deformation in shape recovery process. Compression with 90% strain and cyclic compression experiments were therefore carried out to characterize the mechanical performance. After 90% strain compression, no distinguishable volume change or obvious damage of our aerogel is observed; the compression result is shown in Fig.7a.Just like other kinds of foam materials, the 90% compression curve shows a nonlinear elasticity regime and the curve can be roughly divided into three stages. In the first stage, the strain is lower than 20%, the aerogel shows a nearly linear compression behavior with a modulus of 17.8 KPa caused by the deformation of cell walls. In the second stage, the strain is higher than 20% and less than 60%, the stress will increase slowly to 7 KPa which can be ascribed to the collapse of cell walls. In the last stage, the strain is higher than 60%, the stress will rapidly increase to 55 KPa due to densification process of aerogel. The cyclic compression curve (100 circles) is shown in Fig.7b. As Fig.7b shows, though there will be some structure damage caused by fatigue accumulation and structural defects, the aerogel can still recover its original shape, which means the structure of our aerogel can withstand large deformation. From the results shown in Fig.7b, the cyclic compression stress-strain curve can also be divided into two stages during the loading process. For instance, for the first circle compression curve, when the strain is lower than 20%, the aerogel showed a linear-elastic regime with a modulus of 5 KPa. When the strain is between 20% and 50%, our aerogel shows a nonlinear elasticity with a steeper slope of the stress-strain curve. The maximum modulus at this stage is approximately 10 KPa. There would be a hysteresis loop in every compress circle. Shrinking in the hysteresis loop is observed with the increasing number of cycles. The biggest constriction happens at the 10th circle and the

maximum stress in this loop decreased by 10% compare to the first loop.

To qualify as an effective conductive scaffold in the shape memory composite, the aerogel itself should also have a high electrical conductivity. The electrical conductivity of the proposed aerogel was detected by the four-probe method and the highest average electrical conductivity was found to be 16.30 S/m (Fig.8). Such a high electrical conductivity suggests that most contact points in the tested aerogel sample are made of graphene sheets with relatively low thickness as discussed in the previous sections. Comparisons between aerogels with different CNTs oxide load show that with the increasing weight ratio between CNT oxide and GO, the average electrical conductivity of the aerogel initially increases from 4.97 S/m to 16.30 S/m and subsequently decreases to 12.52 S/m as also shown in Fig.8. The conductivity change can be attributed to two main factors: first, the reduced carbon nanotube will bridge the defects in RGO sheets and increase their conductivity due to their ability to work as nanowires; second, the reduced CNT carbon nanotubes adhering to graphene sheets will act as ribs preventing the agglomeration of the graphene sheets, thus the thickness of graphene sheets decreases and so does the interlayer contact resistance. An excessive amount of the CNT load was found to hinder the contact among graphene sheets and hence lead to the decrease of conductivity. Besides, compared with the conductivity of corresponding aerogel scaffolds, the composite shows a lower conductivity. However, both of them show a similar conductivity variation trend with regard to the variations of the weight ratios of the CNTs oxide and GO. It is reasonable to assume that the fragile structure of compound aerogel is very sensitive to the vacuum infusion process and its structure partially damaged, resulting in the decrease of the conductivity of composites.

Though the conductivity of the composite is lower than the conductivity of the corresponding aerogel, it still shows a 13-orders-of-magnitude increase compared to that of the pure epoxy with an average electrical conductivity around 1×10^{-13} S/m. The highest conductivity value measured for the proposed composite is 5.2 S/m which is superior to that of traditional composites by directly mixing the powdery graphene with the polymer. The high electrical conductivity of our composites should be attributed to the preformed interconnected 3D structure of the aerogels since the load of graphene and CNTs in the composites presented in this work is lower than 1% by weight (weight ratio of aerogel in G20, G40, G60 and G80/epoxy composite corresponds to 0.5 wt%, 0.6 wt%,0.7 wt%, 0.8wt%)

To illustrate the importance of the interconnected 3D structure, conductivity measurements of samples with damaged structure prepared by stirring the mixture of aerogel and epoxy resin before curing were carried out. The conductivity of the samples with damaged structure decreases sharply to 1×10^{-8} S/m, confirming the vital role the preformed 3D structure played in the resultant high conductivity of our composites.

The dynamic-mechanical analysis was operated to evaluate the viscoelastic properties of the cured composites, results are shown in Fig.9. As is shown in Fig.9a, there is only one peak emerged at every tanσ ~ temperature curve, meaning a compatibility between the aerogel and epoxy resin. The corresponding temperature at the peak site shown in the tanδ ~ temperature curve should be assigned to the glass transition temperature (T_g) of the composites. From the obtained results, it is clear that the T_g value of each composite is close to that of the pure epoxy resin (EP), and temperature

difference between composites and pure epoxy resin will diminish with the increase of CNT content in the compound aerogels. According to Wang et al[22], the T_g of the graphene/epoxy composite depends on the balance of confinement effect and influence on curing reaction. The confinement effect of graphene and CNTs will decrease the mobility of polymer chains in the matrix, increasing the T_g value. Thus, the increase in the reduced carbon nanotubes content in aerogel will increase the T_g value; while the effects of aerogel on curing reaction of epoxy matrix will lead to non-stoichiometric balance between epoxy resin and curing agents, resulting in the reduction of the cross-linking density and decreasing the T_g value.

The storage modulus curves of a series of compound aerogel/epoxy composites with different weight ratios of CNT and graphene are depicted in the Fig.9b. As expected and clearly shown in Fig.9b, at temperature lower than the glass transition temperature, the stiffness (i.e., the storage modulus) of every composite is higher than that of the corresponding matrices, which is probably caused by the confinement effect of graphene and carbon nanotubes. Whereas for temperature higher than the glass transition temperature, their stiffness is lower than their corresponding matrices, which could be attributed to the weakened cross-linking density.

The high conductivity of the described composite enable it to recover its original shape without the use of an external heat source due to its ability to heat itself by directly connecting it to a circuit with a voltage of 60 volts. The shape recovery process of our composites is shown in Fig.10.

As is shown in Fig. 10, the composite will gradually recover its original shape. In particular, the recovery rate is only 0.5 degrees per second during the first 20 s; Subsequently, it gradually increases up to 2.1 degrees per second; Finally, it decrease

to approximately 0 in last 30 seconds since most of stress has been released in the early stage (Fig.11) . The surface temperature map of the sample changing with time was also characterized by an infrared radiation thermometer (Fig.12). As is clearly shown in Fig.12, the average surface temperature of the sample will exceed its T_g in 60 seconds, symbolizing that the inner 3D aerogel scaffold can generate enough heat to guarantee the shape recovery process of the sample. Detail surface structure of composite before and after recovery process was characterized by SEM (Figure 13). As displayed in figure 13, before recovery the surface of composite is divided by various tiny cracks and the outline of those cracks displays similar pattern as aerogel scaffold does (Figure 13a). After recovery, such surface feature has disappeared and most cracks has been closed (Figure 13b), symbolizing that none structural failure has happened during the deformation proecessTo distinguish the effect aerogel scaffold with different composition on shape memory performance of composites, the relationships between recovery ratio and time of bended rectangle composites and pristine epoxy sample were characterized (Fig.12). The conductivities of EP/G20, G40, G60 and G80corresponds to 3.2 S/m, 2.0 S/m, 5.2 S/m, and 3.3 S/m. As is depicted in Fig.12, despite the compositions, the shape recovery behaviors of different samples show the same mode. However, their recovery speeds are quite different. It is found that sample with a high conductivity will recover its shape in short time (68s for EP/G60 with a conductivity of 5.2S/m) ,which is comparable to and the results pristine epoxy resin gained by heating sample at its T_g (62 ℃),sample with a low conductivity will recover its shape in relative long time (138s for EP/G40 with a conductivity 2.0 S/m). The differences should be attributed to the heating power of the composites provided by the inner conductive aerogel scaffold as illustrated in Temperature ~ time curve (Fig.15). As illustrated in Fig.15, the surface temperature of

EP/G60 can reach in 60 seconds is high up to 60 ℃, which is comparable to its T_g (63 ℃), and this should be the reason why its recovery speed can match with that of pristine epoxy recovered under its T_g. Compared with EP/G20, G60 and G80, the recovery duration of EP/G40 is much longer despite the fact that EP/G40 possesses similar heating power as EP/G60 and G80. The phenomenon mainly stems from the uneven temperature distribution of EP/G40 (Fig. 16). From the surface temperature pattern of EP/G40, we can clearly find out that different from other samples the temperature of bended area (middle aera) is the lowest.

4. Conclusion

Graphene and carbon nanotube compound aerogels were synthesized by a novel manufacturing technique consisting of freeze-drying followed by annealing. A shape memory aerogel/epoxy composite with carbon nanotubes and graphene compound aerogel as scaffold and epoxy resin as matrix was prepared via a vacuum infusion method. The obtained composite showed a high conductivity up to 5.2 S/m. Shape memory in the aerogel/epoxy composite samples was successfully observed after connecting them to a circuit with a relative low voltage (60 volts).To the best of our knowledge the samples prepared in this work represent first time that the shape memory effect directly driven by an electrical field has been observed in the polymer-infused conductive carbon scaffolds. The composite material presented in this work is likely a suitable candidate for applications requiring polymer-infused conductive aerogels such as electromagnetic shielding, actuators and thermal sensors.

Acknowledgment

This work is supported by the National Natural Science Foundation of China (No. 51373096) and CAST Foundation (No. 201233). Instrumental Analysis Center of Shanghai Jiao Tong University and National Engineering Research Center for Nanotechnology were sincerely acknowledged for assisting relevant analyses.

Reference

1. Y. Li, H. Wang, L. Xie, Y. Liang, G. Hong and H. Dai, *J. Am. Chem. Soc*, 2011, **133**, 7296-7299.
2. S. Sun, G. Zhang, N. Gauquelin, N. Chen, J. Zhou, S. Yang, W. Chen, X. Meng, D. Geng, M. N. Banis, R. Li, S. Ye, S. Knights, G. A. Botton, T.-K. Sham and X. Sun, *Sci. Rep.*, 2013, **3**.
3. Y. B. Luo, Z. G. Shi, Q. Gao and Y. Q. Feng, *J. Chromatogr A*, 2011, **1218**, 1353-1358.
4. T. S. Sreeprasad, S. M. Maliyekkal, K. P. Lisha and T. Pradeep, *J. Hazard. Mater.*, 2011, **186**, 921-931.
5. H. Wang, Y. Wang, Z. Hu and X. Wang, *ACS Appl. Mater. Inter.*, 2012, **4**, 6827-6834.
6. C. Bao, Y. Guo, L. Song, Y. Kan, X. Qian and Y. Hu, *J. Mater. Chem.*, 2011, **21**, 13290.
7. Y. S. Song and J. R. Youn, *Carbon*, 2005, **43**, 1378-1385.
8. K. V. Maheshkumar, K. Krishnamurthy, P. Sathishkumar, S. Sahoo, E. Uddin, S. K. Pal and R. Rajasekar, *Polym. Compos.*, 2014, **35**, 2297-2310.
9. H. Kim, A. A. Abdala and C. W. Macosko, *Macromolecules*, 2010, **43**, 6515-6530.
10. A. S. Wajid, H. S. T. Ahmed, S. Das, F. Irin, A. F. Jankowski and M. J. Green, *Macromol. Mater. Eng.*, 2013, **298**, 339-347.
11. H. Hu, Z. Zhao, W. Wan, Y. Gogotsi and J. Qiu, *Adv. Mater.*, 2013, **25**, 2219-2223.
12. Y. Li, Y. A. Samad, K. Polychronopoulou, S. M. Alhassan and K. Liao, *Sci. Rep*, 2014, **4**.
13. W. Chen and L. Yan, *Nanoscale*, 2011, **3**, 3132-3137.

14. Y. Liu, C. Han, H. Tan and X. Du, *Mater. Sci. Eng., A*, 2010, **527**, 2510-2514.
15. J. S. Leng, H. B. Lv, Y. J. Liu and S. Y. Du, *Appl. Phys. Lett.*, 2007, **91**, -.
16. W. S. Hummers and R. E. Offeman, *J. Am. Chem. Soc,* 1958, **80**, 1339-1339.
17. Y. Guo, C. Bao, L. Song, B. Yuan and Y. Hu, *Ind. Eng. Chem. Res.*, 2011, **50**, 7772-7783.
18. P. N. Nirmalraj, T. Lutz, S. Kumar, G. S. Duesberg and J. J. Boland, *Nano lett.*, 2011, **11**, 16-22.
19. A. K. Geim and K. S. Novoselov, *Nat. Mater.*, 2007, **6**, 183-191.
20. C.-C. Teng, C.-C. M. Ma, C.-H. Lu, S.-Y. Yang, S.-H. Lee, M.-C. Hsiao, M.-Y. Yen, K.-C. Chiou and T.-M. Lee, *Carbon*, 2011, **49**, 5107-5116.
21. P. H. Tan, W. P. Han, W. J. Zhao, Z. H. Wu, K. Chang, H. Wang, Y. F. Wang, N. Bonini, N. Marzari, N. Pugno, G. Savini, A. Lombardo and A. C. Ferrari, *Nat. Mater.*, 2012, **11**, 294-300.
22. S. Wang, M. Tambraparni, J. Qiu, J. Tipton and D. Dean, *Macromolecules*, 2009, **42**, 5251-5255.

Figures and Tables Captions

Figure 1. Fabrication process of the conductivity-enhanced aerogel/epoxy composite with carbon nanotubes and graphene compound aerogel as scaffold and epoxy resin as matrix.

Figure 2. FTIR spectra of carbon nanotube oxide and graphene oxide.

Figure 3. Stability test of 2mg/ml pristine CNTs and CNTs oxide solution (a); AFM image of single layer graphene sheet (b).

Figure 4. XPS spectra of compound aerogel(weight of CNT oxide/GO is 2:5) before and after reduction (a); C1s spectra of graphene after oxidation (b); C1s spectra of graphene after reduction (c); Raman spectra of graphene before and after reduction (d).

Figure 5. TEM image of carbon nanotube oxide and graphene oxide solution with a ratio of 3:5(a), SEM image of carbon nanotube and graphene compound aerogel with a ratio of 3:5(b).

Figure 6. SEM images of compound aerogel with different weight ratios of carbon nanotube oxide and graphene oxide respectively being: 1:5(a); 2:5(b); 3:5(c); 4:5(d).

Figure 7. Compression curve of compound aerogel (CNTs and graphene weight ratio 3:5) 90% strain compression (a); cyclic compression of compound aerogel (CNTs and graphene weight ratio 3:5).

Figure 8. Conductivity variations of the compound aerogels after annealing and their corresponding aerogel/epoxy composites with regard to the variations of the weight ratios of the CNT oxide and GO.

Figure 9. Dynamic mechanical properties of aerogels enhanced epoxy resin composites: Tan delta (a); Storage modulus (b).

Figure 10. Shape recovery process of the compound aerogel (the weight ratio of carbon nanotube and graphene is 3:5)/epoxy resin composite under voltage of 60 volts.

Figure 11. Conductivity change and recovery rate of composite （CNT oxide/GO ratio 3:5） in the recovery process.

Figure 12. Surface temperature distribution of composite （CNT oxide/GO ratio 3:5） in the recovery process.

Figure 13. Surface morphology of shape memory composite（CNT oxide/GO ratio 3:5） before recovery (a) and after recovery (b)

Figure 14. The relationship of recovery time and recovery ratio

Figure 15. Surface temperature of composites

Figure 16. Surface temperature distribution of composite (20th second)

Tables

Table 1. Formulations of the prepared compound aerogel without pyrolyzation.

Table 1

Specimen	G20	G40	G60	G80
CNT oxide	4	8	12	16
GO	20	20	20	20
PVA	100	100	100	100

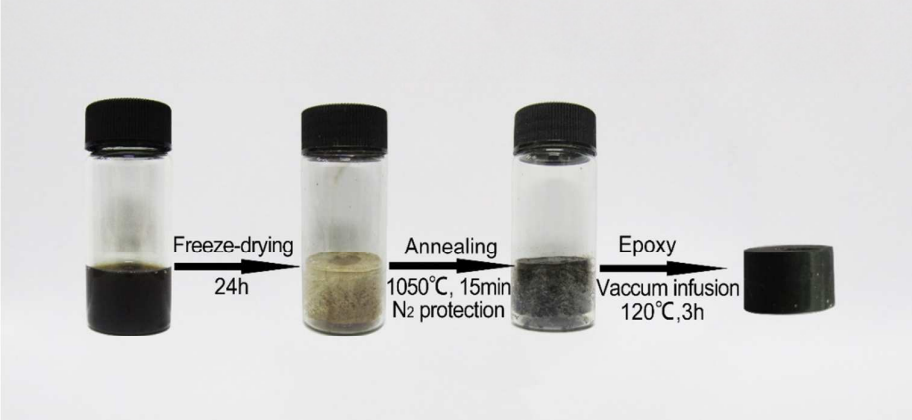

Figure 1

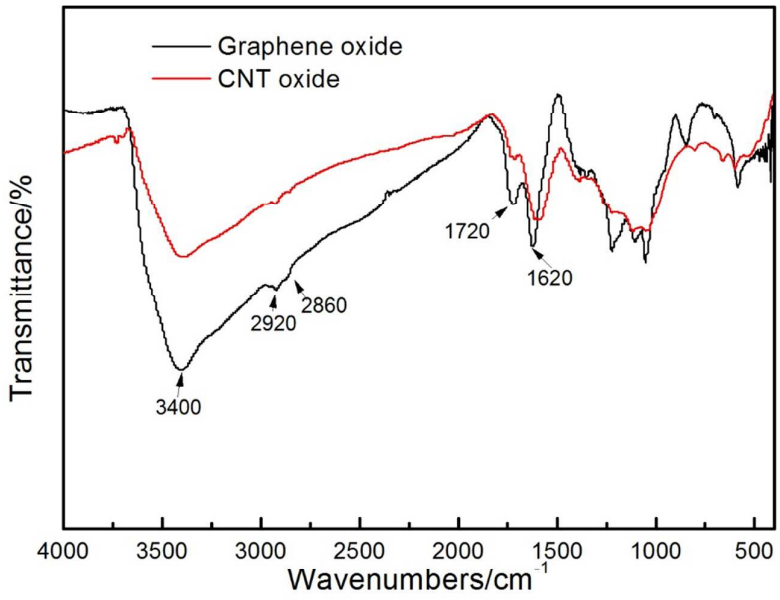

Figure 2

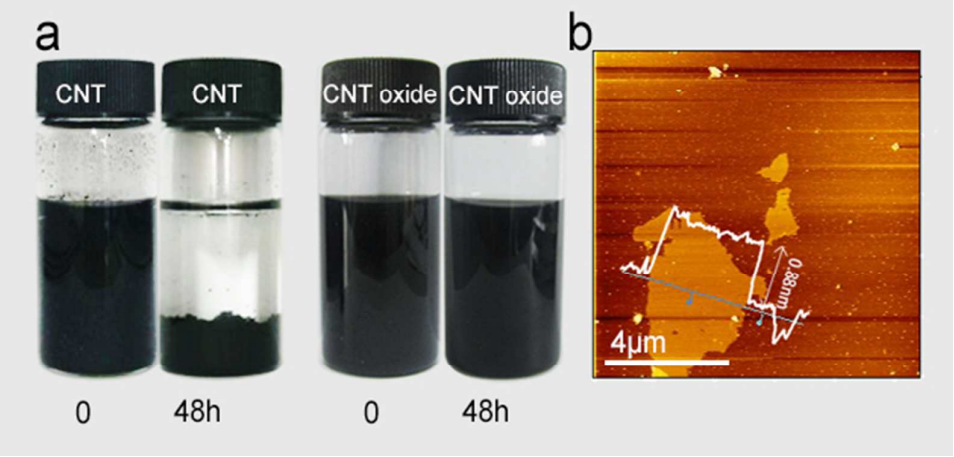

Figure 3

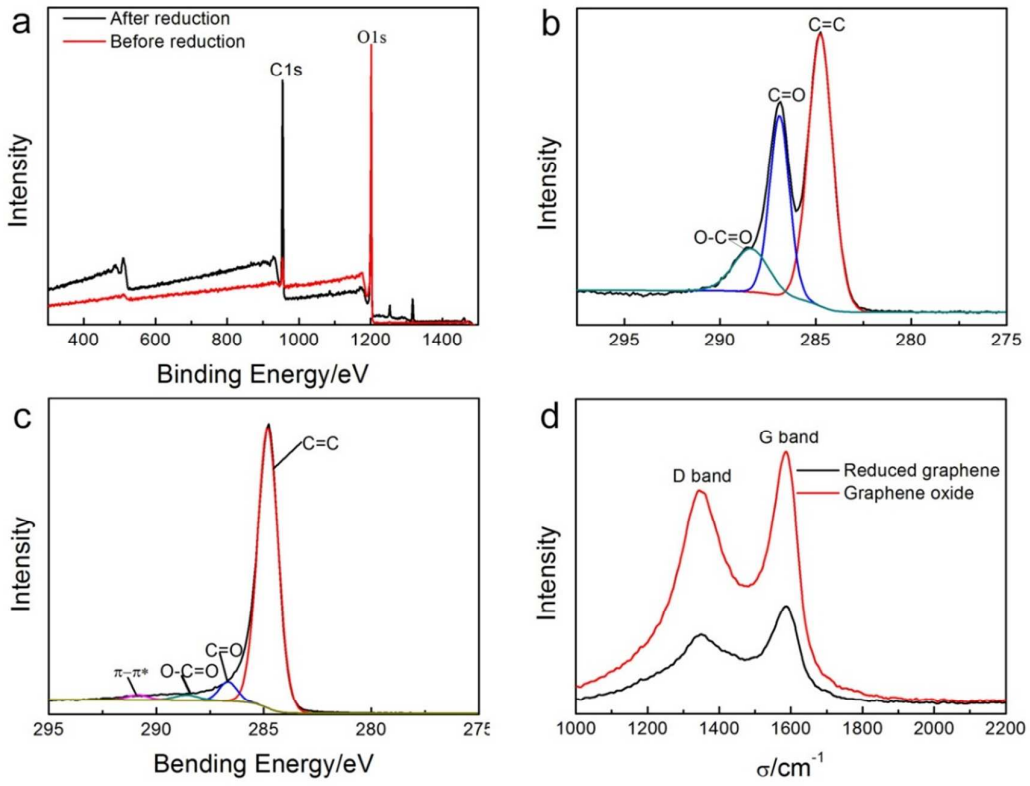

Figure 4

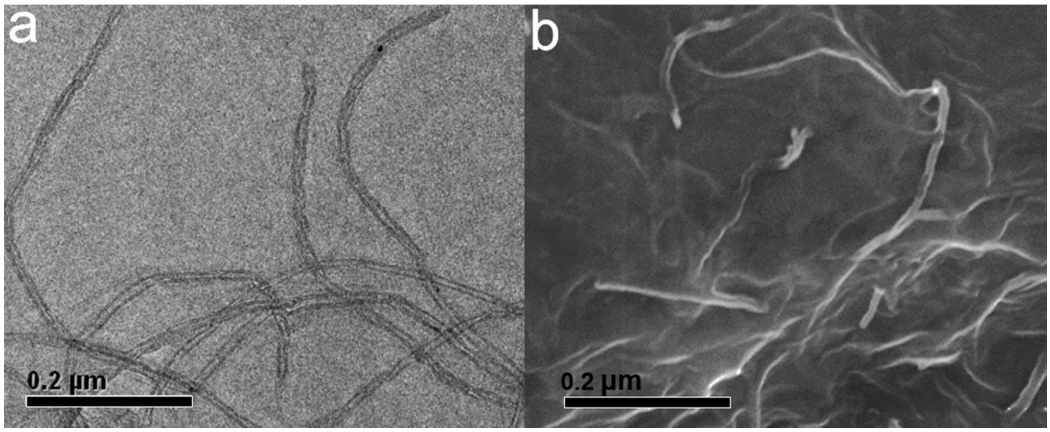

Figure 5

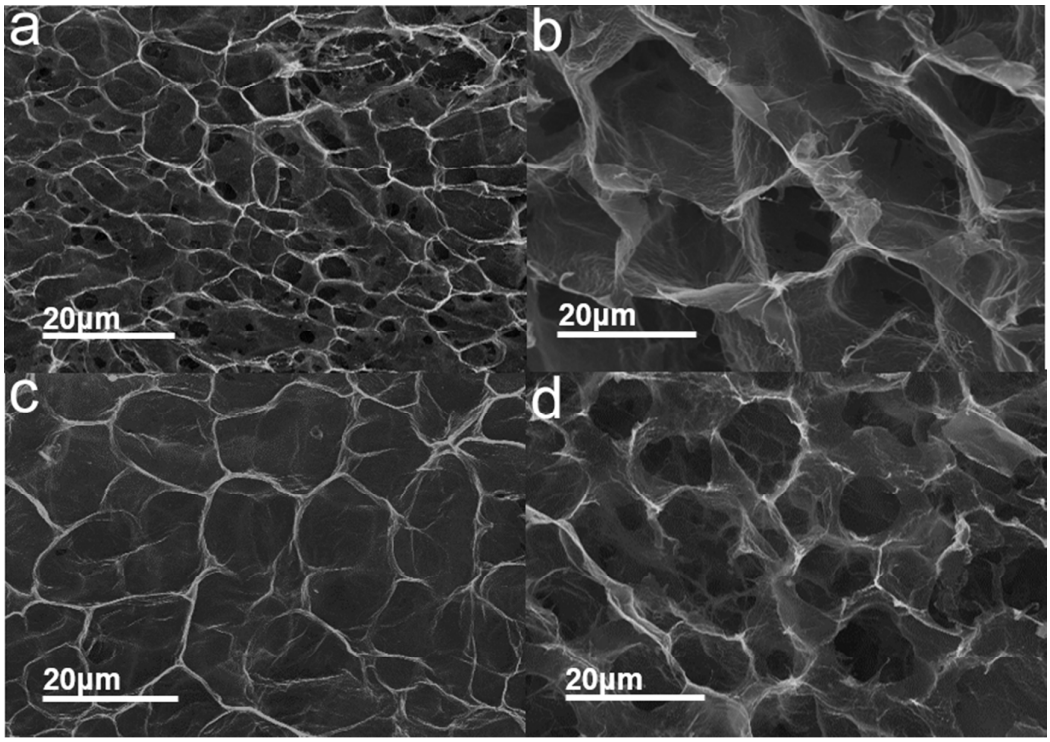

Figure 6

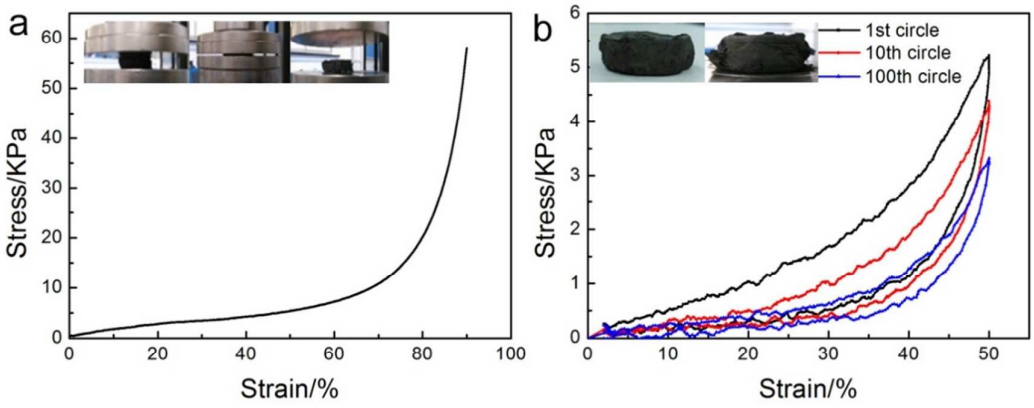

Figure 7

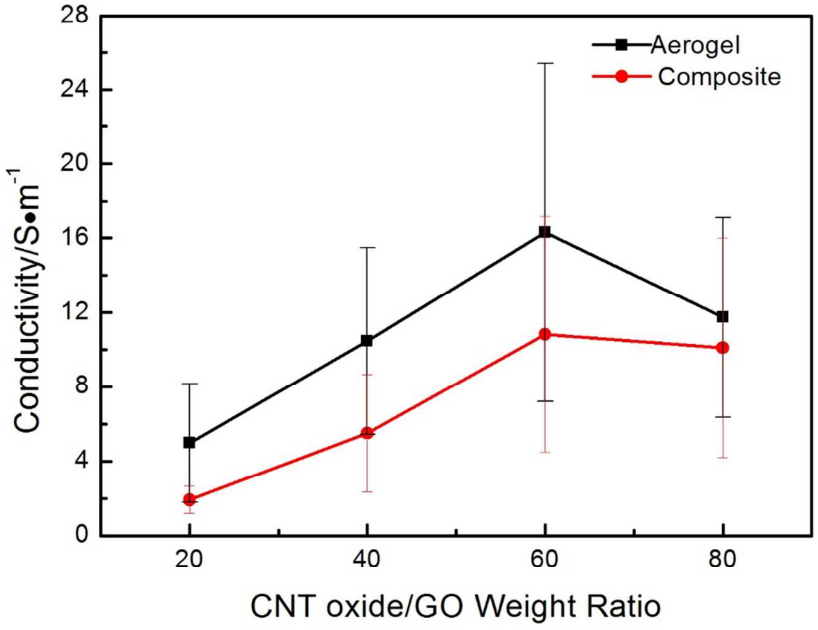

Figure 8

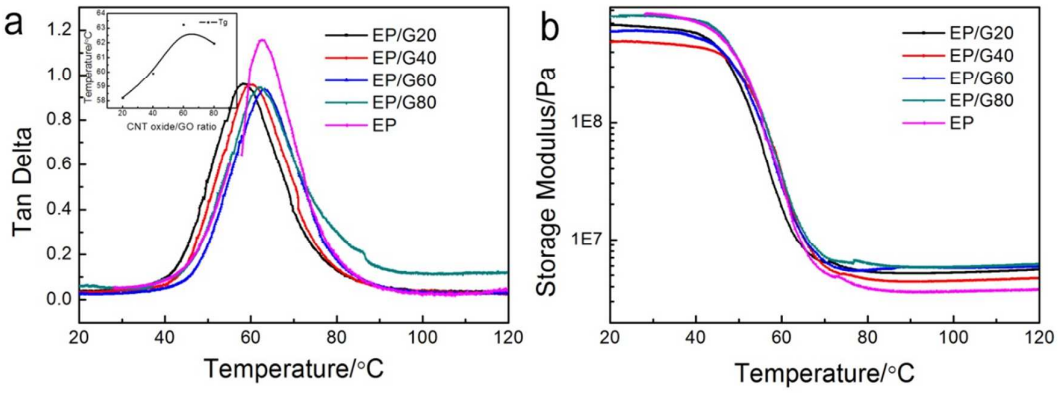

Figure 9

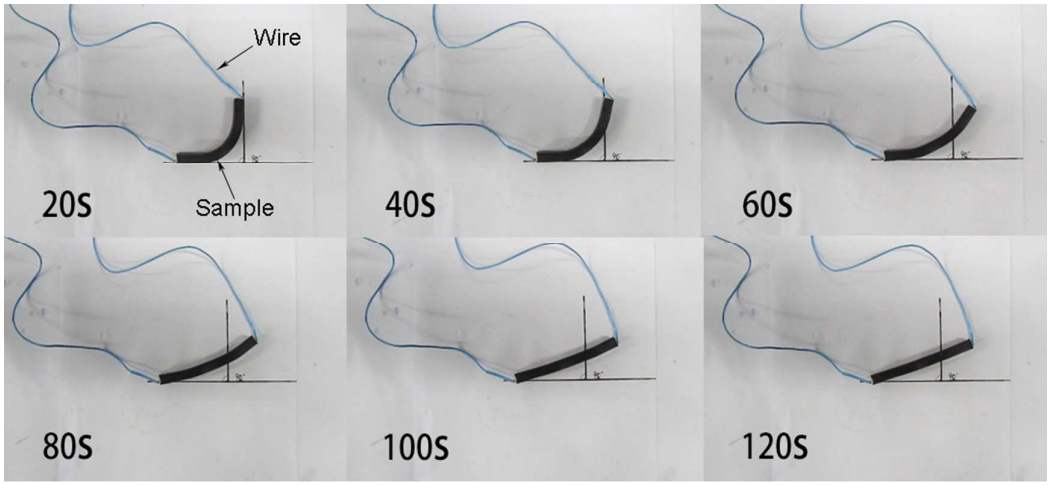

Figure 10

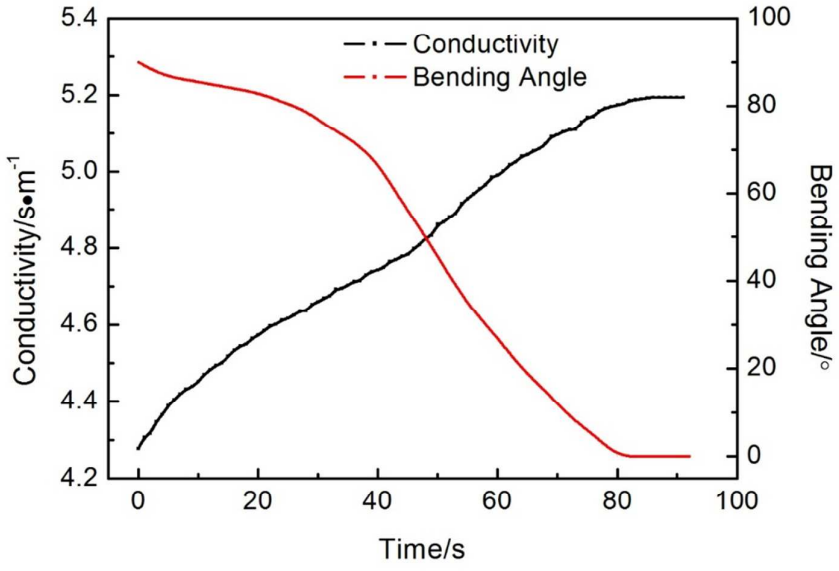

Figure 11

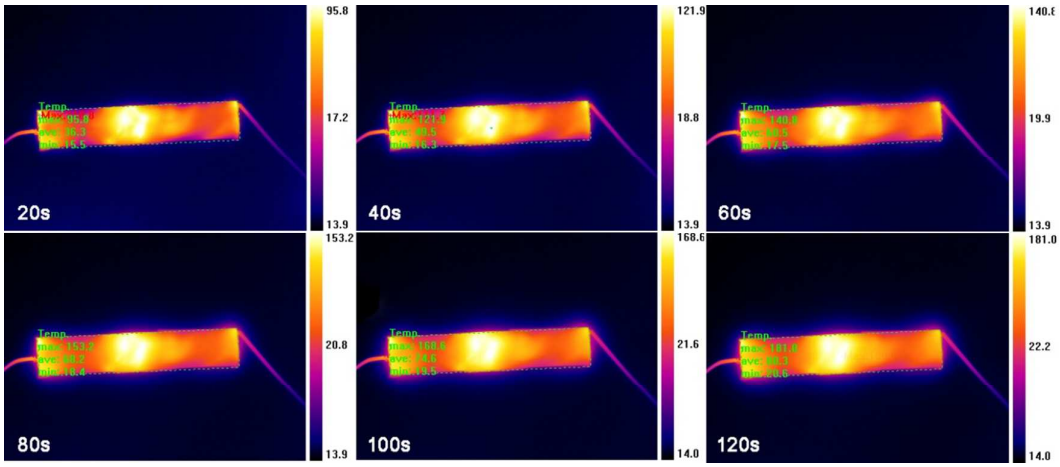

Figure 12

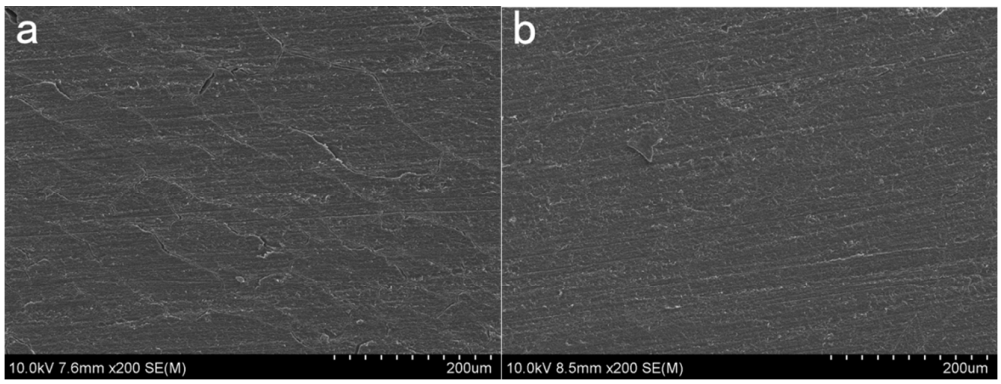

Figure 13

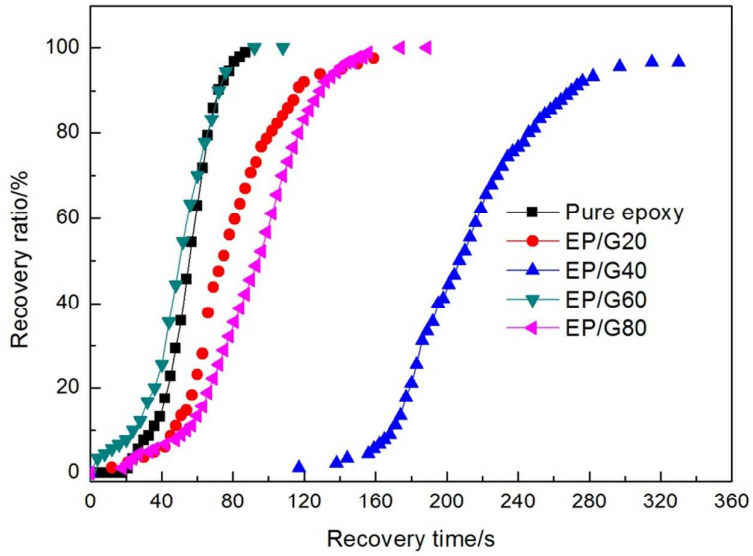

Figure 14

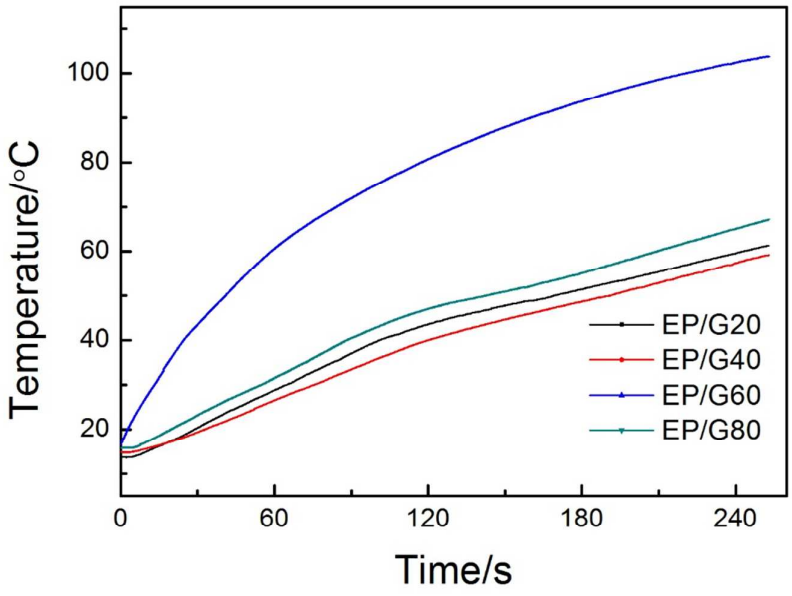

Figure 15

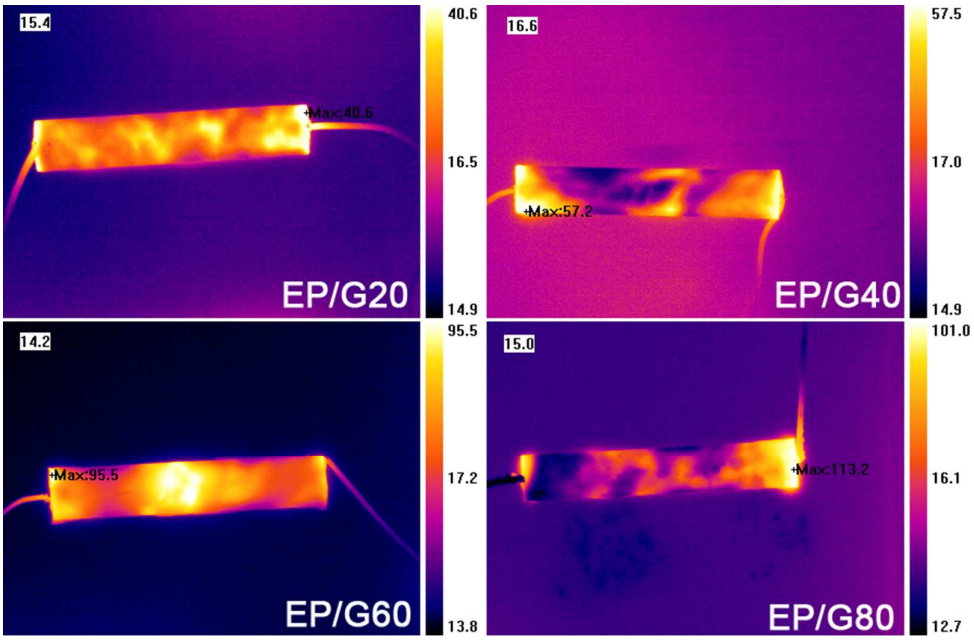

Figure 16